Design and analysis of ultra-wideband microstrip patch antenna with various conductive materials for terahertz gap

Kritika Singh[1] · Marshal Dhayal[2] · Smrity Dwivedi[1]

Abstract

The paper explores the design and analysis of a wideband microstrip patch antenna with a metallic patch and a 3×3 split ring resonator (SRR) array operating in the 0.1–5 THz frequency range. The antenna's structure incorporates different conductive materials such as gold, silver, and graphene as a metallic patch. The dimensions of the metallic patch and SRR are calculated to achieve wideband operation within the desired THz range. The SRR array enhances electromagnetic resonance, thereby improving bandwidth and radiation characteristics for medical imaging. The study discusses the equivalent circuit and design equations for the microstrip patch antenna and SRR unit cell. For designing and analyzing the proposed antenna, CST Microwave Studio 2019 software have been used. Performance parameters such as return loss, bandwidth, gain, efficiency, directivity, VSWR, and radiation pattern have been evaluated. The advantages and limitations of each conductive material are evaluated to determine their suitability for THz-based medical imaging applications. The goal is to maximize the antenna's bandwidth, gain, and image resolution for medical imaging purposes. The findings highlight the performance characteristics of gold, silver, and graphene as conductive materials for medical imaging applications, facilitating the development of high-resolution, non-invasive imaging systems with improved diagnostic capabilities.

Article Highlights

- Microstrip patch antenna loaded with 3×3 Split Ring Resonator for three different conductive materials have been designed and analyzed for medical applications.
- Operating frequency range is 0.1–3 THz.
- CST Microwave Studio 2019 software is used for the simulation of the software.

✉ Kritika Singh, kritikasingh.rs.ece19@iitbhu.ac.in | [1]Department of Electronics Engineering, IIT BHU, Varanasi, UP, India. [2]Department of Physics, IIT Delhi, Delhi, India.

Discover

1 Introduction

The term "medical imaging" encompasses a wide range of techniques used to get visuals of the human body for the purposes of diagnosis, monitoring, and treatment. Several medical technologies provide unique insights about the health of a certain body part, the severity of an injury, or the efficacy of a therapy [1]. Many imaging techniques include X-ray radiography, X-ray CT, MRI, ultrasonography, elastography, optical imaging, radionuclide imaging (Scintigraphy, PET and SPECT, thermography, and terahertz imaging [2]. Terahertz medical imaging is found to be comparatively safer for the biological tissues as compared to other medical imaging techniques due to nonionizing radiations [3], The terahertz region (THz = 10^{12}), as specified by the International Telecommunications Union (ITU), occupies the electromagnetic spectrum from 0.3 to 10 THz [4]. Since it lies in between the infrared and microwave regions, it exhibits characteristics of both. THz has shown to have a tremendous amount of potential in various domains such as high- speed communication [5], medical imaging, material determination [6] and sensing. THz radiation can permeate various materials because of the long wavelength of the THz photons, and it is especially sensitive to the vibration modes of water. It also has some drawbacks, like THz detectors have a low signal to noise ratio and a slow processing speed. The emitters only generate incoherent and dim THz radiation. THz sources require freezing temperatures and a low contrast between healthy and unhealthy tissues [2].

The patch antenna is a prominent form of antenna that has been explored for THz applications. Microstrip antennas have numerous advantages like its compact and light weight patches, high efficiency, operating at short wavelengths, reconfigurability, and dependability. Return loss (which depends on the matching of port and antenna), dielectric loss (depends on the type of material of the substrate used in the antenna) and conductor loss (depends on the type of material used for the conducting patch) are three main factors for designing the microstrip patch antenna [7]. Microstrip patch antennas have some limitations also such as narrow bandwidth, lower gain, low efficiency, back radiation etc. Antenna properties such as gain, bandwidth, and efficiency strongly depend on the material used in the patch, substrate and ground. Employing metamaterials significantly reduces antenna size while simultaneously enhancing bandwidth, gain, and multiband operating frequencies. The concept of a metamaterial was initially proposed by Veselago in 1968 [8]. Many researches have been conducted on the improvement of antenna performance with the introduction of metamaterials, and some encouraging results have been obtained [9]. THz region metamaterial-based antennas have the potential to be useful because of their great penetration with minimal attenuation, nonionizing nature, and remarkable resolution imaging potential [10]. All three antennas are suitable for usage in biomedical applications. Figure 1a illustrates the arrangement of antennas for detecting cancer tumor [11], whereas Fig. 1b demonstrates how an array of antennas may not only detect the tumor but also determine its precise location [12].

A novel DNA shaped fractal antenna with partial ground is designed and proposed for sub-terahertz and terahertz band applications [13]. A plant shaped wideband antenna with partial ground is presented for THz applications [14]. The design of a Vinayak slotted rectangular microstrip patch antenna that offers a quad band resonance with significant characteristics to serve applications including radio determination, satellite, mobile, and space research is proposed in [15]. The improvement in the performance of a novel microstrip patch antenna through added stages of a fractal geometry and a circular split ring resonator for multiband operation is presented in [16]. The design and a detailed discussion of the results of a novel multi
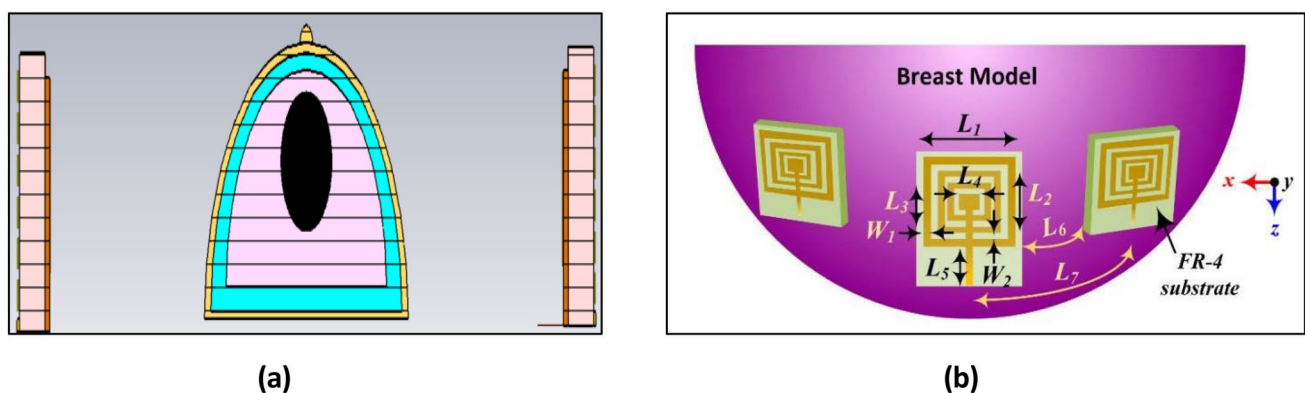

Fig. 1 **a** antennas arrangement for breast tumor detection [11] **b** Antenna array arrangement around the breast [12]

band microstrip patch antenna intended to serve several applications is presented in [17]. A novel Vivaldi antenna for THz medical application in the range of 0.5–2 THz is suggested in [18].

In this paper microstrip patch antennas with three different materials (gold, silver and graphene) are analyzed and compared in the terahertz range. Antennas are designed for the medical imaging applications. In section 2, the design of the antenna has been presented this section is further subdivided into three sections (2.1) Structure and dimensions of the antenna, (2.2) Equivalent circuits and equations of microstrip patch antenna and SRR unit cell. In Sect. 3, Material properties of gold, silver and graphene microstrip antenna, their advantages and limitations of antennas with different materials are discussed. This section is sub divided into three sections, i.e., (3.1) gold microstrip patch antenna (3.2) silver microstrip patch antenna (3.3) graphene microstrip patch antenna. Advantages and limitations of all the three antennas has also been discussed in this section. In Sect. 4, Previous other models are compared with the proposed work. In Sect. 5, Comparison of characteristics of all the three antennas have been presented. Section 6, concludes the paper.

2 Design methodology of the proposed antenna

2.1 Structure and dimensions of the antenna

The proposed structure of antenna has been designed and simulated in CST microwave studio 2019. In the antenna structure, silicon dioxide substrate with the dielectric value of 3.9 and thickness ts, length Ls and width Ws, is sandwiched between the metal radiating patch of thickness tp, length Lp and width Wp and an array of 3×3 SRR with ground of thickness tg. To reduce the back radiation and increase the efficiency, an array of SRR is used. Figure 2 depicts the structure of the proposed antenna.

The distance between each SRR in the array is 70 μm. The antenna structure is designed for the medical imaging range 0.1 THz to 5 THz. The dimensions of the proposed antenna are tabulated in the Table 1 given below.

Resonant frequency can be calculated by Eq. (1) [19]:

$$f_r = \frac{v_0}{\sqrt{2 \times \varepsilon_{eff}}} \frac{4.6 \times 10^{-14}}{g} + \frac{f}{1.01} \tag{1}$$

f_r is resonant frequency, ε_{eff} is effective dielectric constant, v_0 is the electromagnetic wave velocity i.e., 3×10^{11} mm/s, g is the width of the gap or notch, f is the frequency of operation.

$$ts \geq 0.06 \frac{\lambda_{air}}{\sqrt{\varepsilon_r}}$$

ts is the thickness of the substrate, ε_r is dielectric constant of the substrate.

$$W_p = \frac{v_0}{2f_r} \sqrt{\frac{2}{\varepsilon_r + 1}} \tag{2}$$

where, W_p is width of the patch,

$$\varepsilon_{reff} = \frac{\varepsilon_r + 1}{2} + \frac{\varepsilon_r - 1}{2} \left[1 + 12 \frac{t_s}{W_p} \right] \left(\text{where } \frac{W_p}{t_s} > 1 \right) \tag{3}$$

$$\frac{\Delta L}{t_s} = 0.412 \frac{\left(\varepsilon_{reff} + 0.3 \right) \left(\frac{W_p}{t_s} + 0.264 \right)}{\left(\varepsilon_{reff} - 0.258 \right) \left(\frac{W_p}{t_s} + 0.8 \right)} \tag{4}$$

where, ΔL is the normalized extension of length,

$$L_p = \frac{v_0}{2f_r \sqrt{\varepsilon_{reff}}} - 2\Delta L \tag{5}$$

where Lp is the length of the patch, Notch width or width of the gap can be obtained from the following equation,
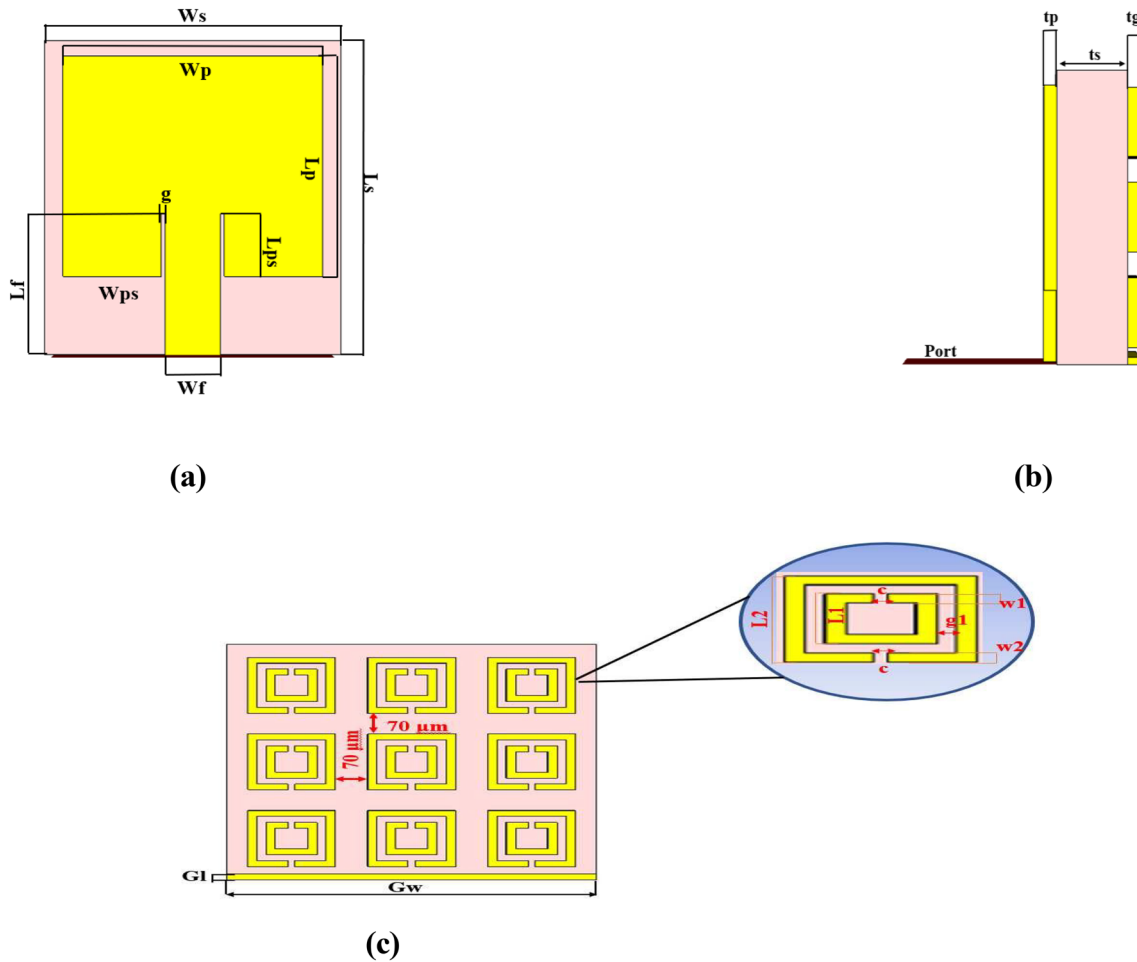
(a)

(b)

(c)

Fig. 2 Design of the antenna **a** patch antenna **b** side view of the antenna **c** enlarged view of the backside

$$f_r = \frac{v_0}{\sqrt{2 \times \varepsilon_{eff}}} \frac{4.6 \times 10^{-14}}{g} + \frac{f}{1.01}$$

For obtaining the preferred resonance at the operating frequency ($f_r = f$),

$$f = \frac{v_0}{\sqrt{2 \times \varepsilon_{eff}}} \frac{4.6 \times 10^{-14}}{g} + \frac{f}{1.01}$$

$$f - \frac{f}{1.01} = \frac{v_0}{\sqrt{2 \times \varepsilon_{eff}}} \frac{4.6 \times 10^{-14}}{g}$$

Or, $f\left(1 - \frac{1}{1.01}\right) = \frac{v_o}{\sqrt{2 \times \varepsilon_{eff}}}$

$$\frac{0.1f}{1.01} = \frac{v_0}{\sqrt{2 \times \varepsilon_{eff}}} \frac{4.6 \times 10^{-14}}{g}$$

$$g = \frac{v_0}{\sqrt{2 \times \varepsilon_{eff}}} \frac{4.6 \times 10^{-12}}{f} \tag{6}$$

Table 1 Dimensions of the proposed antenna

Sl. no.	Parameters	Dimensions (μm)
1	Width of the substrate (Ws)	800
2	Length of the substrate (Ls)	800
3	Thickness of the substrate (ts)	200
4	Width of the patch (Wp)	700
5	Length of the patch (Lp)	560
6	Thickness of the patch (tp)	36
7	Width of the feedline (Wf)	150
8	Length of the feedline (Lf)	360
9	Thickness of the feedline	36
10	Gap (g)	10
11	Length of the outer SRR (L2)	190
12	Width of the outer SRR (W2)	190
13	Length of the inner SRR (L1)	110
14	Width of the inner SRR (W1)	110
15	Width of the ground	800
16	Length of the ground	20
17	Thickness of the ground and SRR (tg)	36
16	Distance between the SRRs	70

2.2 Equivalent circuits and design equations of microstrip patch antenna and SRR unit cell

Equivalent circuits of microstrip patch antenna with inset feed and SRR unit cell are discussed below.

2.2.1 Equivalent circuit and equations of microstrip patch antenna

Figure 3 given below depicts the microstrip patch antenna and its equivalent circuit.
Equivalent of the feed line impedance Z0 can be calculated by the following Eq. (7):

$$Z_0 = R_{in} cos^2 \left(\frac{\pi}{L_p} L_{ps} \right) \tag{7}$$

$$G_1 = \frac{1}{120\pi^2} \int_0^\pi \left[\frac{sin\left(\frac{k_0 W_p}{2} cos\theta \right)}{cos\theta} \right]^2 sin^3\theta d\theta \tag{8}$$

Mutual conductance can be calculated by the following Eq. (9):

$$G_{12} = \frac{1}{120\pi^2} \int_0^\pi \left[\frac{sin\left(\frac{k_0 W_p}{2} cos\theta \right)}{cos\theta} \right]^2 \times J_0\left(k_0 L_p sin\theta \right) sin^3\theta d\theta \tag{9}$$

Here, J0 is the Bessel function of the first kind of order zero. Resonant input impedance can be obtained by the following equation:
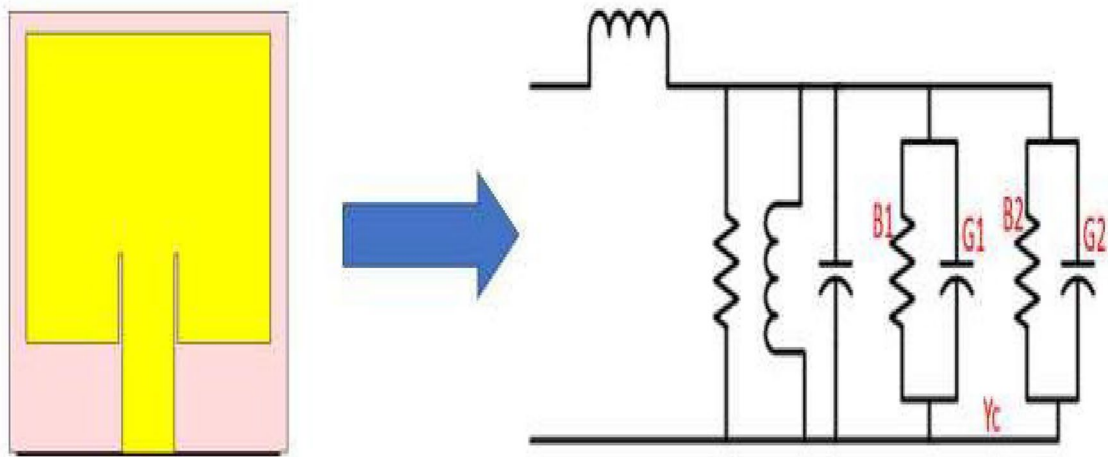
$$R_{in} = \frac{1}{2(G1 + G12)}$$

Fig. 3 Patch antenna and its equivalent circuit [19]

The inset feed causes the formation of a gap or notch, which in turn results in the formation of a junction capacitance. The resonance frequency is affected by this gap or notch and its concomitant junction capacitance.

Here Y is the admittance, G is the conductance and B is the susceptance.

2.2.2 Equivalent circuit and design equations of SRR unit cell

Equivalent circuit of SRR unit cell is shown in the Fig. 4 and design equations for SRR unit cell are discussed below [20].
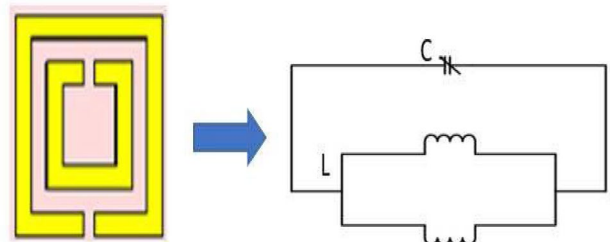
$$\rho = \frac{(N-1)(W+S)}{1-(N-1)(W+S)} \tag{10}$$

$$k = \frac{s/2}{w+s/2} \tag{11}$$

$$C_0 = \varepsilon_0 \frac{k(\sqrt{1-k^2})}{k(k)} \tag{12}$$

$$L_{SRR} = 4\mu_0[L-(N-1)(S=W)]\left[ln\left(\frac{0.98}{\rho}\right)+1.84\rho\right] \tag{13}$$

$$C_{SRR} = \frac{N-1}{2}[2L-(2N-1)(W+S)]C_0 \tag{14}$$

Fig. 4 SRR unit cell and its Equivalent circuit

$$f_{SRR} = \frac{1}{2\pi \sqrt{L_{SRR} C_{SRR}}}$$

(15)

There are two SRR rings, L1 and L2 measuring 190 µm and 110 µm, respectively. The width of each ring is 5 µm. The gap between the slots was 70 µm, and the formulae were used to obtain the capacitance and inductance values for the C_{SRR} and L_{SRR}. The f_{SRR} can determined, for N = 2. A 50-ohm impedance microstrip line inset feed is used to excite the antenna because it offers better impedance matching.

3 Microstrip patch antennas with different materials

Dimensions of all the three antennas are same. Silicon dioxide is used as the substrate in all the antennas. Material properties of gold, silver and graphene microstrip antenna, their advantages and limitations of antennas with different materials are discussed in this section.

3.1 Microstrip patch antenna with gold

In this antenna gold has been used as metal patch at the front side as well as in the array of 3×3 SRR and ground. Substrate is of silicon dioxide which has been sandwiched between both of them.

Gold used in microwave devices due to its high electrical conductivity and simple processing; both of the reasons are facilitated by the fact that it is chemically inert in ambient environments. The amount of current needed to charge a circuit with a constant capacitance value increases as the operating frequency increases [21]. Gold is preferred in terahertz antenna as it does not change its properties in higher terahertz range also. Gold is opted as the radiating material for the antenna in order to make it resistant to corrosion and chemically stable. Gold possesses a significant electrical conductivity at THz frequencies despite having a lesser skin depth (~ 75 nm at 1 THz). Conventional methods of deposition, including as sputtering, evaporation, and electroplating with a high melting point, can be employed without much complication to deposit it on a surface [22]. Using Electron beam lithography THz antenna can be fabricated. After the sanitizing the sample, the photoresist is spun onto the wafer as part of the fourth phase of the manufacturing process. The design is then imported employing the EBL then the last phase is the metal rollout [23]. Properties of gold is depicted in Table 2 given below.

3.1.1 Advantages and limitations of gold

Advantages of Gold:

- Good conductivity: Gold is highly conductive, allowing for efficient signal propagation and enhancing overall antenna performance.

Table 2 Material properties of gold

Parameter	Value
Electron mobility	42.6 cm^2 V^{-1} s^{-1}
Density	19,300 kg/m^3
Tensile strength	120 MPa
Thermal conductivity	34 Wm^{-1} K^{-1}
Electrical resistivity	0.022 µΩ
Heat capacity	0.13 [kJ/K/kg]
Diffusivity	0.00012502 m^2/s
Young's modulus	78 kN/mm^2
Poisson's ratio	0.42
Skin depth	~ 75 nm at 1 THz
Electrical conductivity	4.11 × 107 S/m

- Thermal stability: Gold exhibits excellent thermal stability, making it suitable for terahertz applications where temperature variations can occur.
- Low Ohmic Losses: Gold exhibits relatively low ohmic losses in the terahertz frequency range. This characteristic minimizes the absorption and dissipation of the electromagnetic energy, leading to higher radiation efficiency and reduced signal attenuation.
- Compatibility with Terahertz Frequencies: Gold's material properties make it well-suited for operation in the terahertz regime, where it offers good impedance matching and resonance characteristics. It can facilitate the design and optimization of terahertz microstrip patch antennas.

Limitations of gold:

- Cost: Gold is an expensive material compared to other metals, potentially increasing the overall manufacturing cost.
- Increased Surface Roughness Effects: In the terahertz regime, surface roughness becomes more critical as the wavelength decreases. Gold, being a relatively soft material, can have surface roughness effects that impact the antenna's performance.
- Fabrication Challenges: Fabricating microstrip patch antennas with high precision in the terahertz regime can be challenging. The small dimensions and intricate structures required for terahertz operation pose difficulties in accurately depositing and patterning gold on the substrate, potentially affecting the antenna's performance.

3.2 Microstrip patch antenna with silver

This antenna is made up of silver metal patch and silver 3×3 SRR array and a ground. Substrate is of silicon dioxide which is sandwiched between both of them.

Silver is widely used THz antennas because of its high conductivity and highly conductive materials ensures the enhancement of gain, bandwidth, efficiency etc. [24]. Use of silver in metamaterials at the ground reduces the back radiation hence improving the efficiency of the antenna [25]. Properties of silver is depicted in Table 3 given below.

3.2.1 Advantages and limitations of silver

Advantages of silver:

- Excellent conductivity: Silver is highly conductive, even at terahertz frequencies. Its high conductivity allows for efficient signal propagation, minimizing losses and enhancing the overall antenna performance.
- Low ohmic losses: Silver exhibits low ohmic losses in the terahertz frequency range. This characteristic helps to reduce absorption and dissipation of the electromagnetic energy, resulting in higher radiation efficiency and lower signal attenuation.

Table 3 Material properties of silver

Parameter	Value
Electron mobility	$\sim 56 \, \mathrm{cm^2 \, V^{-1} \, s^{-1}}$
Density	$10.8 \times 10^3 \, \mathrm{kg/m^3}$
Tensile strength	140 MPa
Thermal conductivity	$34 \, \mathrm{Wm^{-1} \, K^{-1}}$
Electrical resistivity	$0.022 \, \mu\Omega$
Heat capacity	0.23 [kJ/K/kg]
Diffusivity	$0.00017764 \, \mathrm{m^{2/s}}$
Young's modulus	$76 \, \mathrm{kN/mm^2}$
Poisson's ratio	0.37
Skin depth	~ 63 nm at 1 THz
Electrical conductivity	$6.173 \times 10 7 \, \mathrm{S/m}$

- Wide bandwidth: The use of silver in the microstrip patch antenna with SRR array can contribute to wider operating bandwidth. Silver's conductivity and surface properties enable improved impedance matching and resonance characteristics, allowing for broader frequency coverage.
- Compatibility with Terahertz Frequencies: Silver is well-suited for terahertz operation due to its material properties. It offers good impedance matching and resonance characteristics, facilitating the design and optimization of terahertz microstrip patch antennas.
- Fabrication Flexibility: Silver is a relatively robust and durable material, making it easier to work with during the fabrication process. It can withstand higher temperatures and mechanical stresses, simplifying manufacturing steps such as soldering, bonding, or etching.

Limitations of silver:

- Cost: While silver is generally less expensive than gold, it is still more costly than other commonly used metals like copper or aluminum. The higher cost of silver may impact the overall manufacturing expenses, particularly in large-scale production.
- Surface roughness effects: In the terahertz regime, surface roughness can significantly affect antenna performance. Silver, being a relatively soft material, may have surface roughness effects that contribute to scattering losses and reduced radiation efficiency.
- Environmental sensitivity: It is sensitive to environmental factors such as moisture or harsh conditions. Additional protective measures or coatings may be necessary to ensure long-term stability and reliability in challenging environments.

3.3 Graphene microstrip patch antenna

This antenna is made up of graphene patch and graphene 3×3 SRR array and a ground. Substrate is of silicon dioxide which is sandwiched between both of them.

The propagation of surface plasmon polariton (SPP) wave is graphene's most interesting new characteristic when measured at THz frequency [26]. Graphene is often characterized as an infinitely thin conductive sheet with a complicated surfaces conductivity for terahertz frequencies [27]. The surface conductivity of graphene may be altered by varying either the electrostatic bias or the chemical doping, which optimizes the graphene THz antennas characteristics [28]. Properties of the graphene are depicted in Table 4 given below.

3.3.1 Advantages and limitations of graphene

Advantages of graphene:

- High carrier mobility: Graphene's exceptional electron mobility allows for fast and efficient electron transport, improving signal response and reducing losses.
- Broadband operation: Graphene's electrical properties enable microstrip patch antennas with wide operating bandwidths, offering greater frequency coverage.

Table 4 Material properties of graphene [29]

Parameter	Value
Electron mobility	$\sim 2\times 10^5$ cm^2 V^{-1} s^{-1}
Current density	$\sim 10^9$ A cm^{-1}
Velocity of fermion	$\sim 10^6$ m s^{-1}
Thermal conductivity	~ 5000 Wm^{-1} K^{-1}
Tensile strength	~ 1.5 Tpa
Breaking strength	42 N m^{-1}
Transparency	$\sim 97\%$
Elastic limit	$\sim 20\%$
Surface area	~ 2360 m^2 g^{-1}

- Tunability: The conductivity of graphene can be adjusted, allowing dynamic control of the antenna's performance, such as changing resonant frequency or adjusting impedance matching.
- Low weight and flexibility: Graphene's ultrathin and lightweight nature make it suitable for weight- conscious and flexible antenna designs.
- Compatibility with CMOS technology: Graphene can be integrated with CMOS technology, enabling the development of integrated antenna systems on a single chip.

Limitations of graphene:

- Limited conductivity: Graphene's intrinsic conductivity is lower than traditional metals, potentially resulting in higher resistive losses and reduced radiation efficiency.
- Fabrication challenges: Fabricating high-quality graphene films and transferring them onto substrates with precise control can be complex and challenging.
- Environmental sensitivity: Graphene's properties can be influenced by factors like moisture, temperature, and contaminants, requiring proper encapsulation or protective coatings.
- Cost: Graphene production and processing can be expensive, potentially limiting its practicality for some applications or industries.

4 Comparison the proposed antenna with previous models

The comparison between the operating frequency, material used, gain, bandwidth, and type of the antenna with previous designed antenna is the THz spectrums are presented in the Table 5 given below. As it can be observed from the table given below that max. gain and bandwidth is obtained in the current wok.

5 Comparative analysis of the characteristics of the three antennas

Visual and tabulated comparative analysis of the characteristics like return loss, gain, radiation efficiency, VSWR, 2D and 3D radiation pattern of all the three antennas (gold, silver and graphene) are given below.

Above Fig. 5 depicts the return loss (S11) for all the three materials i.e., gold, silver and graphene. It can be observed that all the three antennas are ultra-wideband band antennas, so the range of operation is very large. Gold microstrip patch antenna has a bandwidth of 181.97% and minimum return loss is obtained at − 37.27 dB at 1.72 THz. Silver microstrip patch antenna has a bandwidth of 182.02% and minimum return loss is obtained at − 49.43 dB at 4 THz. Whereas graphene has a bandwidth of 180.72% and minimum return loss is obtained at − 60.5 dB at 1.08 THz.

Table 5 Comparison table

| Sl. no.		Operating frequency	Material used	Type of antenna	Bandwidth	Gain
1	This work	0.1–5 THz	Gold	microstrip patch with 3×3 SRR	181.97%	23.16 (dBi)
2	This work	0.1–5 THz	Silver	microstrip patch with 3×3 SRR	182.02%	22.42 (dBi)
3	This work	0.1–5 THz	Graphene	microstrip patch with 3×3 SRR	180.72%	21.79 (dBi)
4	Ref. [18]	0.5–2 THz	Gold	Vivaldi	120% at 1.25 Thz	8.8 (dBi)
5	Ref. [30]	0.1–3.3 THz	Gold	Log periodic	23% at 3.4 THz	9.94 (dB)
6	Ref. [31]	0.8–2 thz	Graphene	Patch	2%,1.47 THz	2.25 dBi
7	Ref. [32]	1.05 and 1.1 THz	silver	Metamaterial	8.2% at 1.14 THz	3.56 (dBi)
8	Ref. [33]	0.5–1.5	Graphene	Patch	2% 1 THz	11.1 (dBi)
9	Ref. [34]	0.1–2 thz	Graphene	Slot	56% at 0.4, 06 THz	2.1 (dBi)
10	Ref. [35]	0.3–0.8 Thz	Graphene	Yagi-uda	20% 0.48 THz	9.07 (dBi)
11	Ref. [36]	1 to 5 THz	Graphene	Vivaldi	53% at 2.31 THz	6.48 (dBi)
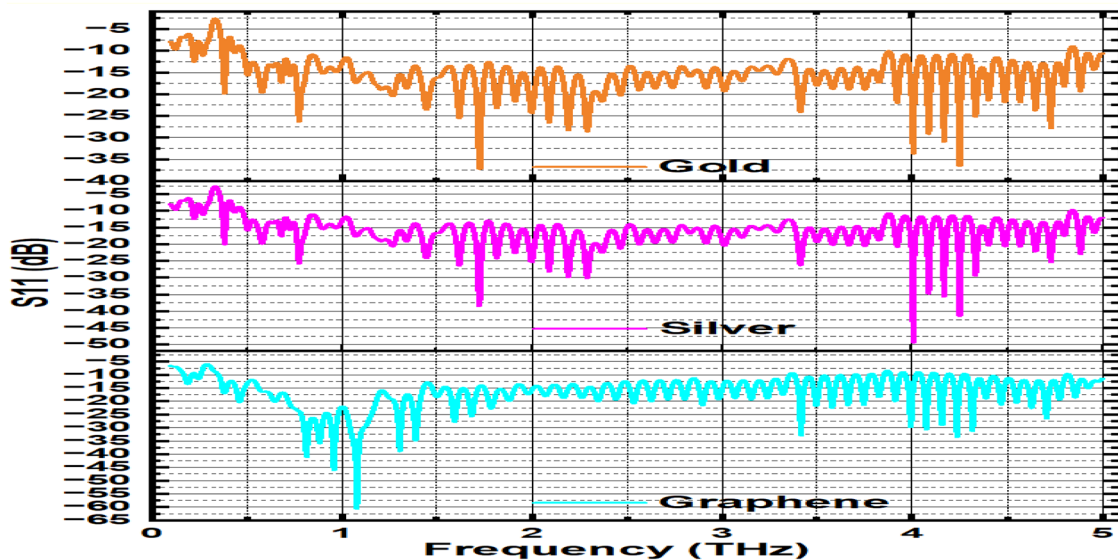
Fig. 5 Return loss of gold, silver and graphene microstrip patch antenna

Above Fig. 6 depicts the gain for all the three materials i.e., gold, silver and graphene. The gain of the gold microstrip patch antenna obtained is 23.16 dBi. The gain of the silver microstrip patch antenna obtained is 22.42 dBi. Whereas the gain of the graphene antenna obtained is 21.79 dBi.

Above Fig. 7 depicts the radiation efficiency for all the three materials i.e., gold, silver and graphene. It can be observed that the radiation efficiency of the gold microstrip patch antenna is 85%. The radiation efficiency of the silver microstrip patch antenna is 78%. Whereas the radiation efficiency of the graphene microstrip patch antenna is 78.1%.

Above Fig. 8 depicts the VSWR for all the three materials i.e., gold, silver and graphene. It can be observed that VSWR of all the three microstrip patch antenna is below 2.

Above Fig. 9a shows the 3D radiation pattern of the gold microstrip patch antenna at 4.5 THz. Whereas 2D radiation of the microstrip patch antenna at 4.5 THz (constant phi) is depicted in Fig. 9b. From the above fig it can be depicted that the side lobe level is at − 14.3 dB and the half power beam width is 17.5 degree (3 dB).
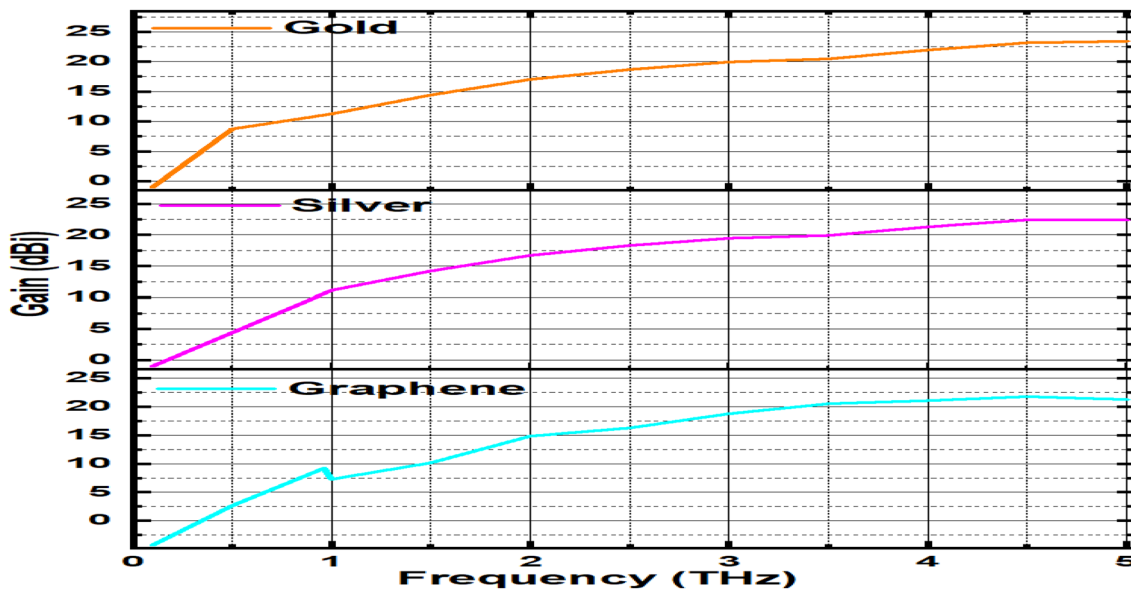

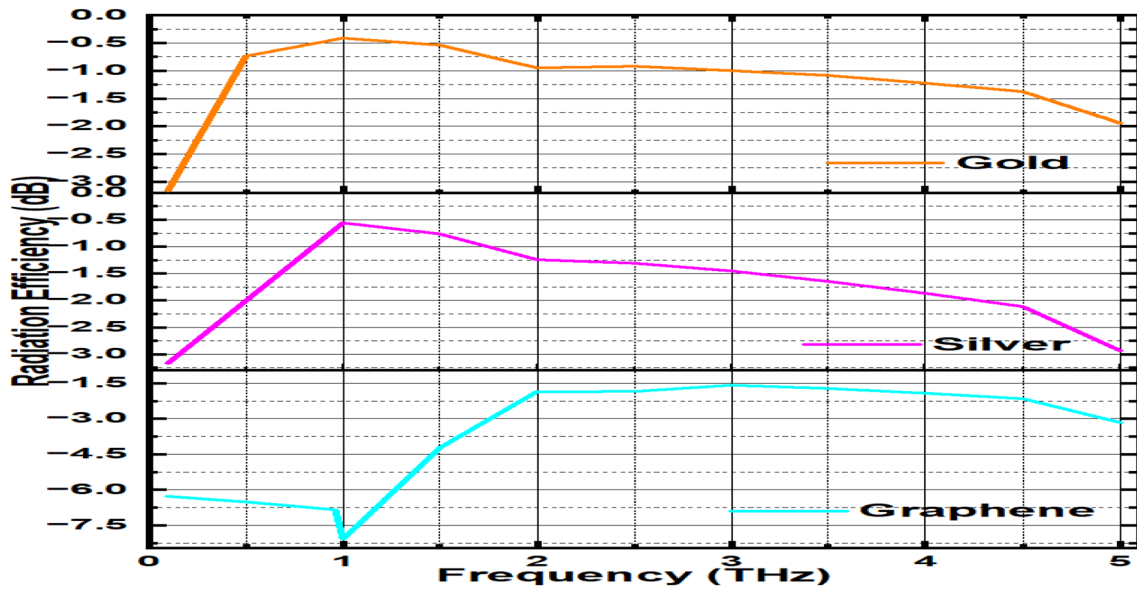**Fig. 6** Gain of gold, silver and graphene microstrip patch antenna

Fig. 7 Radiation efficiency of gold, silver and graphene microstrip patch antenna
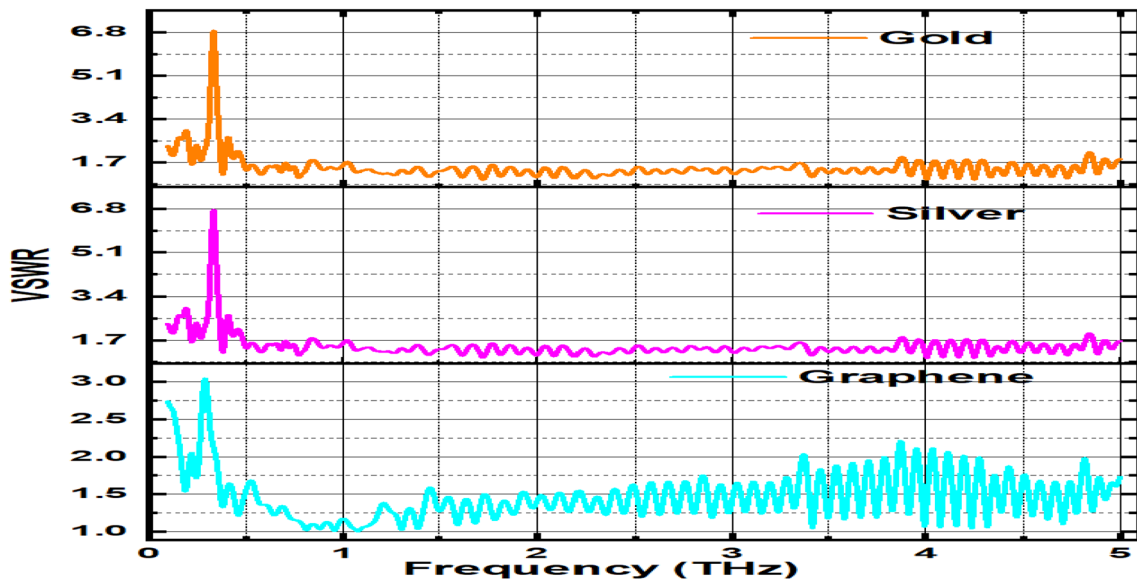

Fig. 8 VSWR of gold, silver and graphene microstrip patch antenna

Figure 10a shows the 3D radiation pattern of the silver microstrip patch antenna at 4.5 THz. Whereas 2D radiation of the microstrip patch antenna at 4.5 THz (constant phi) is depicted in Fig. 10b. From the above fig it can be depicted that the side lobe level is at − 13.9 dB and the half power beam width is 17.5 degree (3 dB).
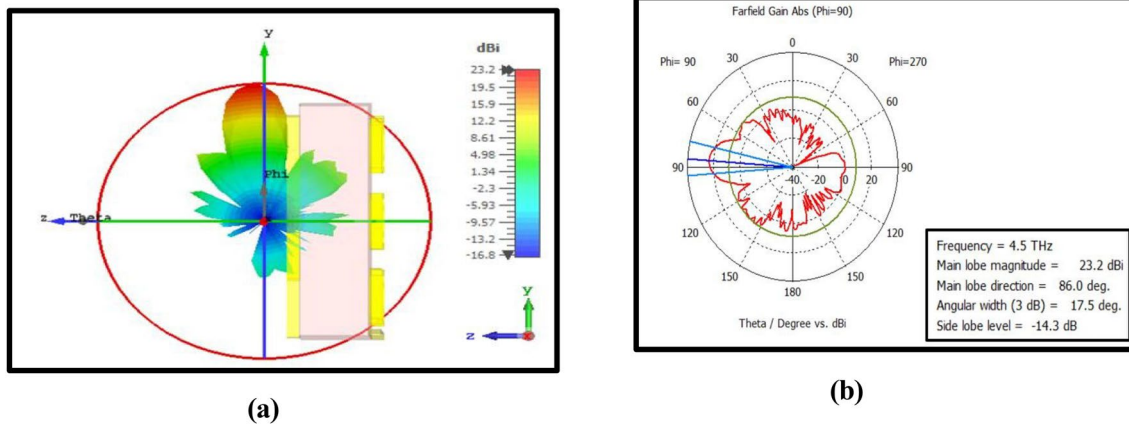
Figure 11a shows the 3D radiation pattern of the graphene microstrip patch antenna at 4.5 THz. Whereas 2D radiation of the microstrip patch antenna at 4.5 THz (constant phi) is depicted in Fig. 11b. From the above fig it can be depicted that the side lobe level is at − 10.4 dB and the half power beam width is 20.7 degree (3 dB).

(a)

(b)

Fig. 9 **a** 3D radiation pattern of gold patch antenna, **b** 2D radiation pattern of gold microstrip patch antenna
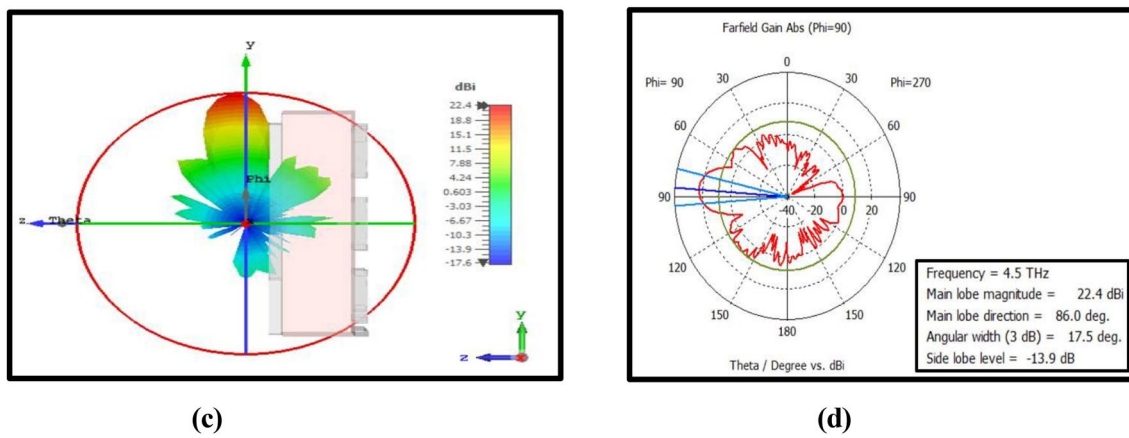

(c)

(d)

Fig. 10 **a** 3D radiation pattern of silver patch antenna, **b** 2D radiation pattern of silver microstrip patch antenna
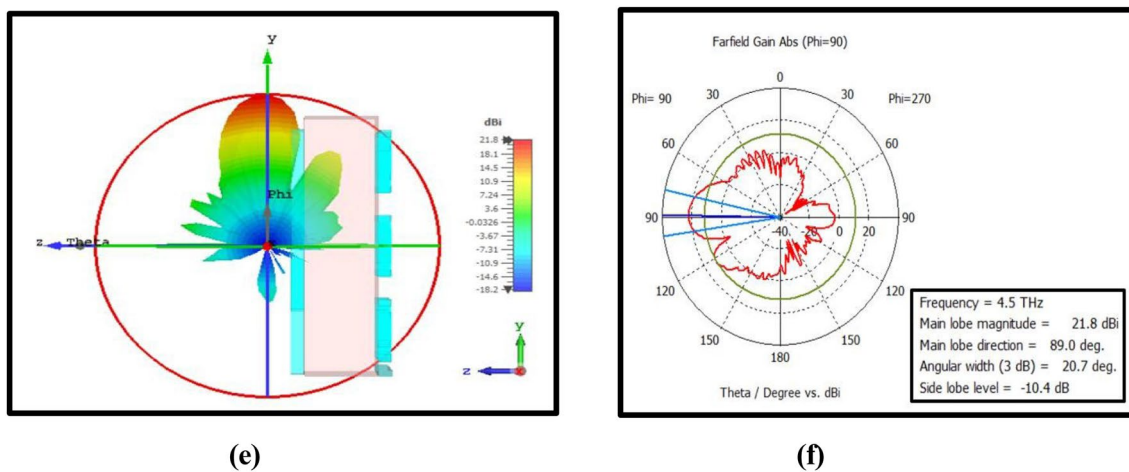

(e)

(f)

Fig. 11 **a** 3D radiation pattern of graphene patch antenna and **b** 2D radiation pattern of graphene microstrip patch antenna

Table 6 Comparison table

Sl. no.	Characteristics	Gold antenna	Silver antenna	Graphene antenna
1	Return loss (min.) (dB)	− 37.27 at 1.72 THz	− 49.43 at 4 THz	− 60 at 1.08 THz
2	Bandwidth (%)	181.97	182.02	180.72
3	Gain (dBi)	23.16	22.42	21.79
4	Efficiency (%)	85	78.41	78.1
5	Directivity (dBi)	24.53	24.53	23.93
6	VSWR	< 2	< 2	< 2
7	HPBW (3 dB)	17.5	17.5	20.7
8	Side lobe level	− 14.3	− 13.9	− 10.4

6 Conclusion

The designs and analysis of all three antennas have been done, and a comparison of their various characteristics can be observed in Table 6 given above. As it can be observed from the aforementioned table, graphene has the lowest return loss in comparison to gold and silver; the bandwidth of silver is larger in comparison to gold and graphene; gold has the maximum gain and efficiency of 23.16 dBi and 85% respectively; VSWR is below 2 in all three cases; the half-power beam width of gold and silver is the same; and graphene has the minimum side lobe level, which is − 14.3. Considering the above-discussed advantages, limitations and characteristics obtained after simulation, the selection of gold, silver, or graphene for a terahertz microstrip patch antenna with SRR arrays should be based on specific application requirements, cost considerations, and the desired trade-offs between performance and fabrication complexity. Since there is a trade-off between the characteristics of the three antennas, any antenna can be utilized as long as it meets the requirements and is appropriate for the medical imaging application.

Author contributions KS: conceptualization, simulation, visualization, writing—original draft, writing—review MD: supervision, writing—review and editing; SD: conceptualization, analysis of the simulated results, validation, methodology, supervision, writing—review and editing.

Data availability All data used for this study are contained in this article.

Declarations

Competing interests The authors have no competing interests to declare that are relevant to the content of this article.

References

1. Center for Devices and Radiological Health & Center for Devices and Radiological Health. Medical Imaging. U.S. Food And Drug Administration. https://www.fda.gov/about-fda/fda-organization/center-devices-and-radiological-health. (Aug 2018)
2. Kasban H, El-Bendary MAM, Salama DH. A comparative study of medical imaging techniques. Int J Inf Sci Intell Syst. 2015;4(2):37–58.
3. Yu L, Hao L. The medical application of terahertz technology in non-invasive detection of cells and tissues: opportunities and challenges. R Soc Chem Adv. 2019;9:9354–63. https://doi.org/10.1039/C8RA10605C.
4. Radwan A, Verri V, D'Amico M, Guido Gentili G. Beam reconfigurable antenna for the THz band based on a graphene high impedance surface. Phys E Low-Dimen Syst Nanostruct. 2017;85:316–23. https://doi.org/10.1016/j.physe.2016.09.015.
5. Jha KR, Singh G. Prediction of highly directive probe-fed microstrip antenna at terahertz frequency. Int J Numer Model Electron Netw Devices Fields. 2012;25(2):175–91. https://doi.org/10.1002/jnm.822.
6. Carelli P, Chiarello F, Castellano MG. THZ discrimination of materials: development of an apparatus based on room temperature detection and metasurfaces selective filters. J Infrared Millim Terahertz Waves. 2017;38(3):303–13. https://doi.org/10.1007/s10762-016-0343-0.

7. Pozar DM. Microstrip antennas. Proc IEEE. 1992;80(1):79–91. https://doi.org/10.1109/5.119568.
8. Veselago VG. The electrodynamics of substances with simultaneously negative values of s and μ. Phys Usp. 1968;10(4):509–14. https://doi.org/10.1070/PU1968v010n04ABEH003699.
9. Krzysztofik WJ, Cao TN, Metamaterials in application to improve antenna parameters. In: Intechopen;2019. https://doi.org/10.5772/intechopen.80636.
10. Mukherjee P, Gupta B. Terahertz (THz) frequency sources and antennas—a brief review. Int J Infrared Milli Waves. 2008;29:1091–102. https://doi.org/10.1007/s10762-008-9423-0.
11. Singh K, Dhayal M, Dwivedi S. Breast cancer detection by terahertz UWB microstrip patch antenna loaded with 6X6 SRR array. IETE J Res. 2023. https://doi.org/10.1080/03772063.2023.2233474.
12. Alibakhshikenari M, Virdee BS, Shukla P, Parchin NO, Azpilicueta L, See CH, Abd-Alhameed RA, Falcone F, Huynen I, Denidni TA, Limiti E. Metamaterial-inspired antenna array for application in microwave breast imaging systems for tumor detection. IEEE Trans Antennas Propag. 2020. https://doi.org/10.1109/ACCESS.2020.3025672.
13. Keshwala U, Rawat S, Ray K. Design and analysis of DNA shaped antenna for terahertz and sub-terahertz applications. Optik. 2021;232:166512. https://doi.org/10.1016/j.ijleo.2021.166512.
14. Keshwala U, Rawat S, Ray K. Plant shaped antenna with trigonometric half sine tapered leaves for THz applications. Optik. 2020;223:165648. https://doi.org/10.1016/j.ijleo.2020.165648.
15. Kaushal D, Shanmuganantham T. A Vinayak slotted rectangular microstrip patch antenna design for C-band applications. Microw Opt Technol Lett. 1833;2017(59):1837. https://doi.org/10.1002/mop.30628.
16. Kaushal D, Shanmuganantham T. Parametric enhancement of a novel microstrip patch antenna using Circular SRR Loaded Fractal Geometry. Alex Eng J. 2018;57(4):2551–7. https://doi.org/10.1016/j.aej.2017.08.021.
17. Kaushal D, Shanmuganantham T. Design of a compact and novel microstrip patch antenna for multiband satellite applications. Mater Today Proc. 2018;5(10):21175–82. https://doi.org/10.1016/j.matpr.2018.06.516.
18. Toolabi M, Khatir M, Naser-Moghadasi M, Amiri N. Vivaldi antenna for early cancer detection based on THz spectroscopy: Comparison between response of breast and skin cancer. Optik. 2023;273:170440. https://doi.org/10.1016/j.ijleo.2022.170440.
19. Matin MA, Sayeed AI. A design rule for inset fed rectangular microstrip patch antenna. WSEA S Transactions on Communications; 2010.
20. Geetharamani G, Aathmanesan T. Metamaterial inspired THz antenna for breast cancer detection. Berlin: Springer; 2019. https://doi.org/10.1007/s42452-019-0601-6.
21. Humpston G. The essential role of gold in the fabrication of microwave electronics systems. Gold Bull. 1999;32:75–9. https://doi.org/10.1007/bf03216613.
22. Walther M, Cooke DG, Sherstan C, Hajar M, Freeman MR, Hegmann FA. Terahertz conductivity of thin gold films at the metal-insulator percolation transition. Phys Rev B. 2007;76(12):125408. https://doi.org/10.1103/PhysRevB.76.125408.
23. Kabashin AV, et al. Nanofabrication with pulsed lasers. Nanoscale Res Lett. 2010;5(3):454–63. https://doi.org/10.1007/s11671-010-9543-z.
24. Haddad M, Jamel N, Nordin AN. Fleible antenna: a review of design, materials, fabrication, and applications. In: Journal of Physics: Conference Series, ICE4CT 2020. https://doi.org/10.1088/1742-6596/1878/1/012068
25. Prahlada Rao K, Vani RM, Hunagund PV. Investigation of effect of silver coating on microstrip antenna arrays. J Appl Electromagn. 2020. https://doi.org/10.12816/0058145.
26. Christensen J, Anjavacas A, Thongrattanasiri MS, Koppens FHL, García de Abajo FJ. Graphene plasmonics: a platform for strong light-matter interactions. ACS Nano. 2012;6:431–40. https://doi.org/10.1021/nl201771h.
27. Hanson GW. Dyadic Green's function and guided surface waves for a surface conductivity model of graphene. J Appl Phys. 2008. https://doi.org/10.1063/1.2891452.
28. Dash S, Patnaik A. Dual band reconfigurable plasmonic antenna using bilayer graphene. In: IEEE International Symposium on Antennas and Propagation AP-S 2017; July 9–14, 2017; San Diego, USA. https://doi.org/10.1109/APUSNCURSINRSM.2017.8072503.
29. Ashyap AY, Zainal Abidin Z, Dahlan SH, Majid HB, Saleh G. Metamaterial inspired fabric antenna for wearable applications. Int J RF Microw Comput Aided Eng. 2018. https://doi.org/10.1002/mmce.21640.
30. Shirzadian Gilan M, Rashed-Mohassel J, Naser-Moghaddasi M, et al. Design of a wideband microstrip nanoantenna array. Opt Quant Electron. 2019;51:132. https://doi.org/10.1007/s11082-019-1852-6.
31. Kazemi F. Dual band compact fractal THz antenna based on CRLH-TL and graphene loads. Optik. 2020;206:164369. https://doi.org/10.1016/j.ijleo.2020.164369.
32. Sirmaci YD, Akin CK, Sabah C. Fishnet based metamaterial loaded THz patch antenna. Opt Quant Electron. 2016;48:168. https://doi.org/10.1007/s11082-016-0449-6.
33. Seyedsharbaty MM, Sadeghzadeh RA. Antenna gain enhancement by using metamaterial radome at THz band with reconfigurable characteristics based on graphene load. Opt Quant Electron. 2017;49:221. https://doi.org/10.1007/s11082-017-1052-1.
34. Kazemi F. High Q-factor compact and reconfigurable THz aperture antenna based on graphene loads for detecting breast cancer cells. Superlattices Microstruct. 2021;153:106865. https://doi.org/10.1016/j.spmi.2021.106865.
35. Tabatabaeian ZS. Graphene load for harmonic rejection and increasing the bandwidth in Quasi Yagi-Uda array THz antenna for the 6G wireless communication. Opt Commun. 2021;499:127272. https://doi.org/10.1016/j.optcom.2021.127272.
36. Bansal G, Marwaha A, Singh A. A graphene-based multiband antipodal Vivaldi nanoantenna for UWB applications. J Comput Electron. 2020;19:709–18. https://doi.org/10.1007/s10825-020-01460-2.

Discover